

Dissolution of Sodium Halides by Confined Water on Au(111) *via* Langmuir–Hinshelwood Process

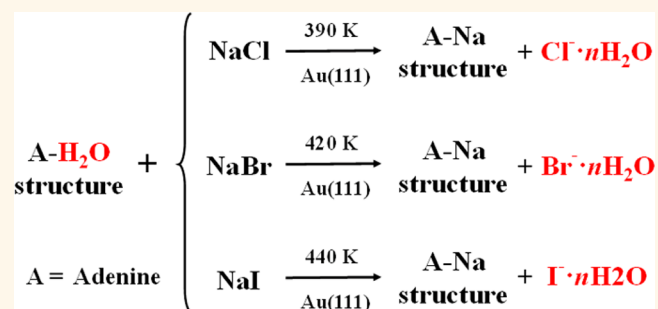
Yuanqi Ding, Xinyi Wang, Donglin Li, Lei Xie, and Wei Xu*¹

Interdisciplinary Materials Research Center, College of Materials Science and Engineering, Tongji University, Shanghai 201804, People's Republic of China

S Supporting Information

ABSTRACT: Salt dissolution is generally encountered in widespread phenomena in nature. As a typical case, the dissolution of NaCl has been widely investigated in aqueous environment, while the process and mechanism of the on-surface dissolution may differ from that in solution and remain to be explored. Herein, we model a NaCl dissolution process on the Au(111) surface with confined water at room temperature (RT) and above. With the assistance of adenine molecules as water reservoir and carrier, the dissolution of NaCl is achieved above RT *via* the Langmuir–Hinshelwood mechanism rather than the Eley–Rideal one, along with the selective formation of stable Cl[−] hydrates, which desorb from the surface in the next step. To explore the generality, such a strategy has been extended to other sodium halide systems (*e.g.*, NaBr and NaI), and expectedly, the dissolution of sodium halides is also achieved by forming stable Br[−] and I[−] hydrates *via* the Langmuir–Hinshelwood process.

KEYWORDS: dissolution of sodium halides, on-surface ion hydration, confined water, Langmuir–Hinshelwood process, scanning tunneling microscopy



Salt dissolution, generally along with the ion hydration process, is fundamentally important to the environment and life.^{1–5} Ion hydration, as a crucial step in the salt dissolution process, plays a vital role in a wide range of areas from basic science to artificial technology, such as biological ion channels,^{6,7} water desalination,⁸ electrochemistry,⁹ and aqueous batteries.¹⁰ As a typical case, the dissolution of sodium chloride (NaCl) with the formation of Na⁺/Cl[−] hydrates has attracted tremendous interest and been widely investigated in both experimental^{11–13} and theoretical studies.^{14–16} On the other hand, the dissolution of NaCl on wet surfaces is particularly interesting, in which the process and mechanism could be different from that in solution. The model system of on-surface salt dissolution could be built up and explored by surface science methods. Under well-controlled ultrahigh vacuum (UHV) conditions, with the assistance of scanning probe microscopy (STM and AFM), Jiang *et al.* achieved the artificial assembly of individual Na⁺ hydrates by means of STM manipulations and moreover provided real-space evidence on the detailed structural information on Na⁺ hydrates at the atomic scale.¹⁷ Furthermore, Jiang *et al.* also tried to probe the dissolution process of the Au(111)-supported NaCl islands by a 2D ice overlayer below the freezing point. It was shown that after increasing the sample temperature to 155 K (at which

water molecules completely desorb from the surface), the dissolved NaCl island was found to recrystallize on Au(111).¹⁸ Based on the above, it is therefore of utmost interest and challenge to mimic the on-surface NaCl dissolution with confined water at RT and above, with the aim of exploring the process of the formation of ion hydrates, more importantly, to unravel the fundamental mechanism of ion hydration on a metal surface.

Generally, most reactions that take place at the gas–solid interface are classified in terms of two proposed mechanisms, that is, the Eley–Rideal (ER) and the Langmuir–Hinshelwood (LH) processes.^{19–21} The ER process refers to a process in which a species from the gas phase enters the surface region and finds an adsorbed species with which to react and generate the product. This process essentially depends on the gas–surface collision, in which a gas-phase species reacts directly with an adsorbate. The LH process refers to a process in which two species enter the surface region, adsorb on the surface, further interact with each other during the random migration

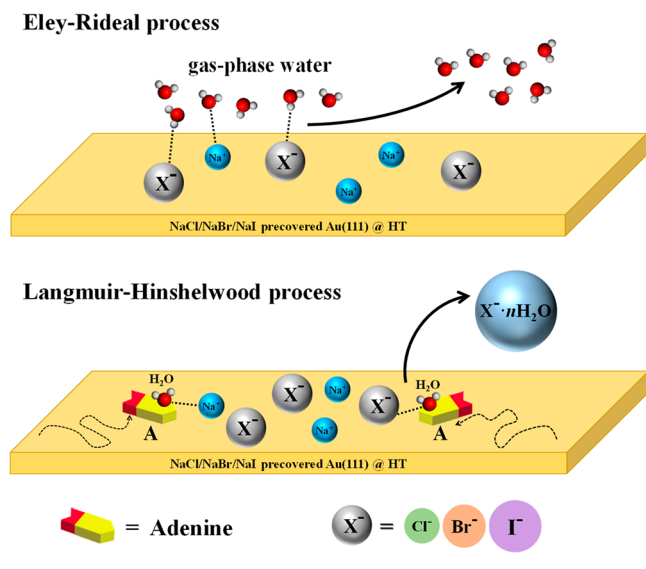
Received: March 22, 2019

Accepted: May 3, 2019

Published: May 3, 2019

on the surface, and generate the product. This process occurs between two accommodated species, in which the reactants initially coadsorb on the surface and are in thermal equilibrium with the substrate. To understand the mechanism of dissolution of NaCl at the surface, consequently, we tried to perform both ER and LH processes on a noble Au(111) surface, respectively. First, we heated the NaCl-precovered surface at different temperatures from room temperature (RT) to ~ 500 K (the thermal treatment ensured the dissociation of Na^+ and Cl^- on the surface^{22–25}) under a water environment at a pressure of ~ 0.001 mbar. As water molecules can hardly adsorb on the Au(111) surface above RT,^{26,27} they may only interact with the dissociated Na^+ and Cl^- ions from the gas phase directly, as occurs in the Eley–Rideal process (cf. Scheme 1), while it was found that the NaCl square lattice was

Scheme 1. Schematic illustration of the proposed dissolution of sodium halides (NaCl, NaBr, NaI) via the Eley–Rideal process (upper panel) and the Langmuir–Hinshelwood process (lower panel). The formation and desorption of stable halide ion hydrates are achieved with A-molecule-confined water via the Langmuir–Hinshelwood process.



not perturbed and there is even no erosion of edges of NaCl islands (as shown in Figure 1), which thus indicates that the dissolution of NaCl via the ER process seems unfeasible.

It is then natural to perform the experiment and explore the possibility of NaCl dissolution via the LH pathway, in which, importantly, water molecules have to be adsorbed on the “hot” surface. Therefore, it is necessary to construct a “reservoir” that enables the confinement of water molecules on the surface. Inspired from our previous study on the interactions between water and organic molecules,²⁸ we found that it is possible to form water-involved structures with A molecules (i.e., A-H₂O structures) via hydrogen bonds, where water molecules can be trapped and carried by A molecules on the Au(111) surface and even released from the A-H₂O structure via thermal treatments due to the intrinsic dynamics of hydrogen-bonded structures. The adenine molecule is thus suitable to be employed as the water reservoir.

Herein, with the assistance of A molecules, we successfully bring water molecules from the gas phase onto the surface as

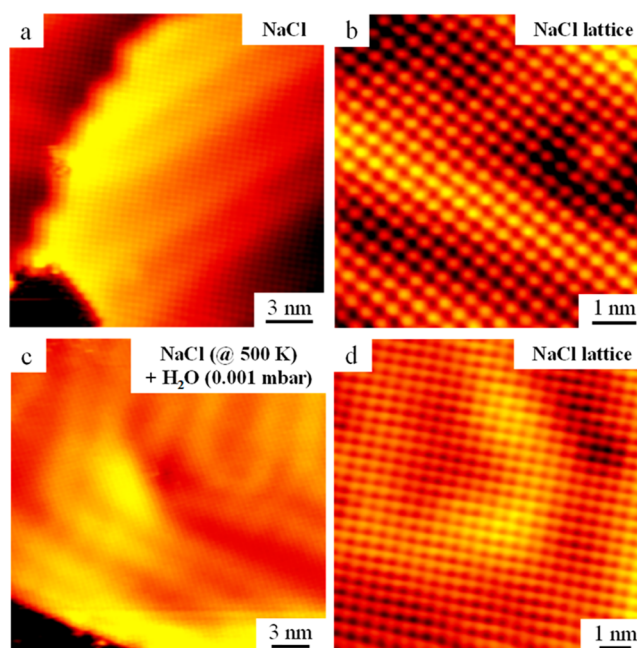


Figure 1. STM images showing the undissolved NaCl on Au(111) during the ER process. (a) Large-scale and (b) close-up STM images showing the overview and the atomic-scale lattice of the NaCl island before exposing to the water environment. (c) Large-scale and (d) close-up STM images showing the overview and the atomic-scale lattice after annealing the sample at 500 K under a water environment at a pressure of ~ 0.001 mbar.

adsorbates, and after annealing the A-H₂O and NaCl covered surface at 390 K, to our surprise, it is found that the formation of the A-Na structure prevails on the surface, and meanwhile, the NaCl islands vanish. The comparative experiment shows that after annealing A and NaCl covered surface at 390 K without introduction of water results in the phase separation of A and NaCl structures, which thus indicates that dissolution of NaCl (i.e., formation and desorption of stable Cl^- hydrates) via the LH process is achieved (cf. Scheme 1). To further explore the possibility of the formation of Na^+ hydrates, we expose the A-Na structure under the water environment and then anneal the sample at 400 K; however, it is found that the A-Na structure is still preserved, which indicates that formation of stable Na^+ hydrates does not seem possible. In order to extend such a strategy to other salts, we further introduce NaBr and NaI to explore the universality. As a result, expectedly, we find that dissolution of sodium halides by forming stable Br^- and I^- hydrates via the LH process is also achieved. This systematic study mimics the on-surface salt dissolution by bringing water molecules from the gas phase to a surface-confined state (binding with A molecules via hydrogen bonds), and in such a condition, we demonstrate the process of ion hydration through the selective formation of stable halide ion hydrates via the LH process in an efficient and global manner.

RESULTS AND DISCUSSION

After co-deposition of NaCl and A molecules on the Au(111) surface held at RT, it is observed that the NaCl and A molecules keep their own self-assembled structures,^{29,30} which are separated on the surface (as shown in Figure 2a). After subsequently exposing such a sample (held at RT) to the water environment at a pressure of ~ 0.001 mbar, it leads to the coexistence of NaCl islands and A-H₂O structures²⁸ (as shown

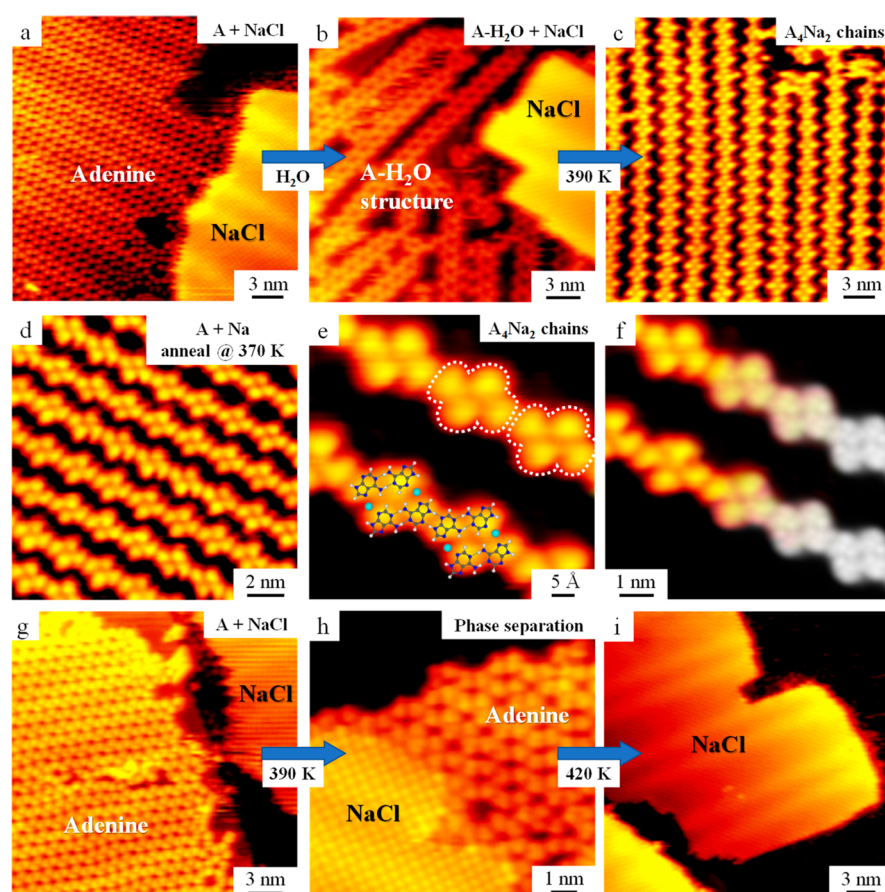


Figure 2. (a–c) STM images showing the dissolution of NaCl on Au(111) above RT *via* the LH process. (a) STM image showing the phase separation of A and NaCl structures on Au(111) at RT. (b) STM image showing the coexistence of the A-H₂O structure and NaCl island after exposing the sample (held at RT) to a water environment at a pressure of ~ 0.001 mbar. (c) STM image showing the formation of the A₄Na₂ chains after annealing the sample at 390 K. (d–f) Formation of the A₄Na₂ chains after deposition of an A molecule and Na on Au(111) followed by annealing at 370 K. (d) Large-scale STM image showing the overview of A₄Na₂ chains. (e) Close-up STM image partially superimposed with the DFT-optimized gas-phase model. The individual A₄Na₂ motifs are depicted by white contours. Hydrogen bonds are depicted by blue dashed lines. H: white; C: gray; N: blue; Na: light blue. (f) High-resolution STM image partially superimposed with the STM simulation (the gray parts) at a bias voltage of -1.2 V. (g–i) STM images showing the phase separation of A and NaCl structures after annealing the sample step by step up to 420 K until the desorption of A molecules from the surface.

in Figure 2b). As reported previously,²⁸ water molecules within the A-H₂O structure could be released *via* thermal treatment above 350 K. After further annealing the sample to 390 K, surprisingly, chain structures are formed, as shown in Figure 2c, and more amazingly, the NaCl islands vanish at such a relatively low temperature. With the insufficient water dosing at a pressure of 1×10^{-5} mbar and annealing at 390 K, adenine islands, NaCl islands, and the chain structures are found to coexist on the surface as shown in Figure S1.

A further comparative experiment of A molecules interacting with sodium on Au(111) provides more information to understand this structural transformation. Directly depositing Na onto the A-covered surface and annealing at 370 K, interestingly, we observe the formation of characteristically the same chain structures (*cf.* Figure 2d) as the ones shown in Figure 2c. From the close-up STM image (*cf.* Figure 2e), we are able to identify that this molecular chain is periodically composed of tetrameric motifs as indicated by white contours. Based on the experimental observations, density functional theory (DFT) calculations are performed, and the optimized structural model (Figure 2e) together with the STM simulation (the gray parts shown in Figure 2f) are partially superimposed on the STM images, respectively. We thus assign

this tetrameric motif to an A₄Na₂ structure, in which electrostatic interactions between A-Na and hydrogen bonds between A–A are distinguished from the DFT model. The elementary A₄Na₂ motifs are further linked with the neighboring ones *via* double NH \cdots N hydrogen bonds, forming the chain structure. This A₄Na₂ chain structure is stable on the surface until its desorption at 450 K. On the basis of the above experimental results, it is natural to attribute the chain structure shown in Figure 2c to be composed of A₄Na₂ motifs.

To further explore the structural constituent on the surface in Figure 2c, that is, to determine if Cl ions are still on the surface, we then perform another control experiment by simply depositing A and NaCl on the surface and annealing the sample step by step without introduction of water. As shown in Figure 2g–i, it is observed that A and NaCl structures keep the phase separation after annealing at 390 K, and A molecules desorb from the surface at 420 K, leaving the NaCl islands alone. Such an experiment shows that A and Na⁺ cannot form the above observed A-Na chain structure when Cl[−] is present on the surface; instead, due to the strong interaction between Na⁺ and Cl[−], formation of NaCl islands is predominant. From the above, we could determine that Cl ions should be absent in the situation shown in Figure 2c. On the other hand, it was

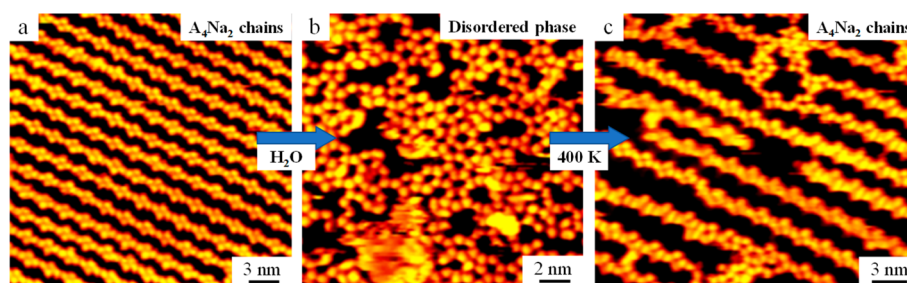


Figure 3. STM images showing that the A_4Na_2 chains are still preserved after exposing the surface to the water environment and then annealing. (a) STM image showing the formation of A_4Na_2 chains. (b) STM image showing the formation of a disordered phase after exposing the sample (held at RT) to the water environment at a pressure of ~ 0.001 mbar. (c) STM image showing the re-formation of A_4Na_2 chains after annealing at 400 K.

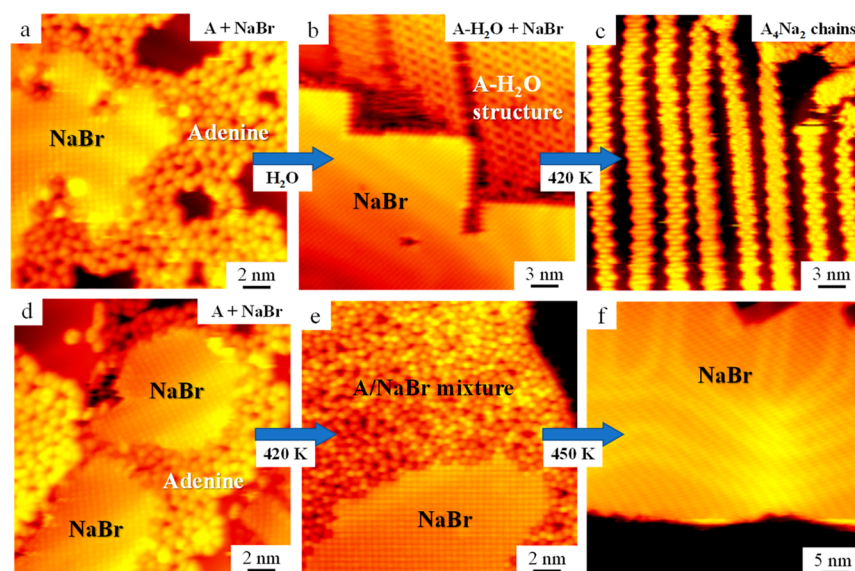


Figure 4. (a–c) STM images showing the dissolution of NaBr on Au(111) above RT *via* the LH process. (a) STM image showing the phase separation of A and NaBr structures on Au(111) at RT. (b) STM image showing the coexistence of the A- H_2O structure and NaBr island after exposing the sample (held at RT) to the water environment at a pressure of ~ 0.001 mbar. (c) STM image showing the formation of the A_4Na_2 chains after annealing at 420 K. (d–f) STM images showing the formation of an A/NaBr mixture phase after annealing the A and NaBr precovered sample at 420 K and the desorption of A molecules from the surface at 450 K.

shown that halogens normally desorb from the Au(111) surface at temperatures above 500 K^{20,31–34} (also *cf.* Figure 1). Therefore, it is rational to speculate that water molecules should facilitate the desorption of Cl ions from the surface by forming stable Cl^- hydrates. At this point, we could safely draw the conclusion that the dissolution of NaCl through surface-confined water molecules *via* the LH process is achieved (also *cf.* Scheme 1).

Theoretical studies on NaCl dissolution^{14–16} with a liquid water film inferred that the anion's preferential dissolution is due to its polarizability, which is in good agreement with our experiment in which NaCl is dissolved on the Au(111) surface along with the formation and desorption of stable Cl^- hydrates. The next question arises: can we achieve the formation of Na^+ hydrates? After exposing the A_4Na_2 chain structures (*cf.* Figure 3a) to the water environment at a pressure of ~ 0.001 mbar, it leads to the formation of a disordered phase (as shown in Figure 3b). Further annealing the sample to 400 K, however, results in the re-formation of the A_4Na_2 chains (Figure 3c), which suggests that in this process the formation of stable Na^+ hydrates is not achieved.

On the basis of the above experimental results and analysis, we reasonably speculate the possible whole scenario of the NaCl dissolution as follows: (i) In the beginning, water molecules are trapped by A molecules forming the A- H_2O structure on the surface. (ii) After annealing above 350 K, A- H_2O motifs are released from the island structure and diffuse on the surface; meanwhile the thermal treatment at this temperature enables the dissociation of NaCl into Na^+ and Cl^- on the surface.^{22–25} Water molecules interact with both Cl^- and Na^+ in specific configurations, *e.g.*, forming $OH\cdots Cl^-$ hydrogen bonds and $O-Na^+$ electrostatic interactions, respectively. (iii) Further annealing at 390 K leads to the formation of the stable Cl^- hydrates most probably due to this specific on-surface hydrogen-bonded configuration among A- H_2O-Cl^- resembling the lever principle (where the O atom toward the surface acts as the “fulcrum”, *cf.* Figure S2). For the A- H_2O-Na^+ configuration, the O atom faces the Na^+ so that formation of the “lever” is not feasible. Therefore, such an on-surface salt dissolution process along with the selective formation of stable Cl^- hydrates is only realized *via* the LH mechanism rather than the ER one.

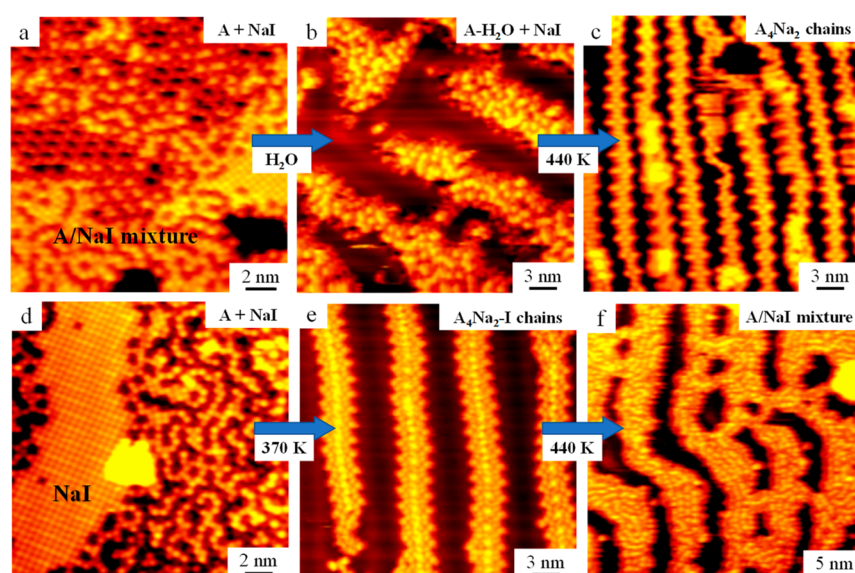


Figure 5. (a–c) STM images showing the dissolution of NaI on Au(111) above RT *via* the LH process. (a) STM image showing the formation of an A and NaI mixture phase after deposition of A and NaI on Au(111) held at RT. (b) STM image showing the formation of an A-H₂O and NaI mixture phase after exposing the sample (held at RT) to a water environment at a pressure of ~ 0.001 mbar. (c) STM image showing the formation of the A₄Na₂ chains after annealing at 440 K. (d–f) STM images showing the formation of A₄Na₂-I chains after annealing an A and NaI precovered sample at 370 K and the A/NaI mixture phase following the herringbone reconstruction of Au(111) at 440 K.

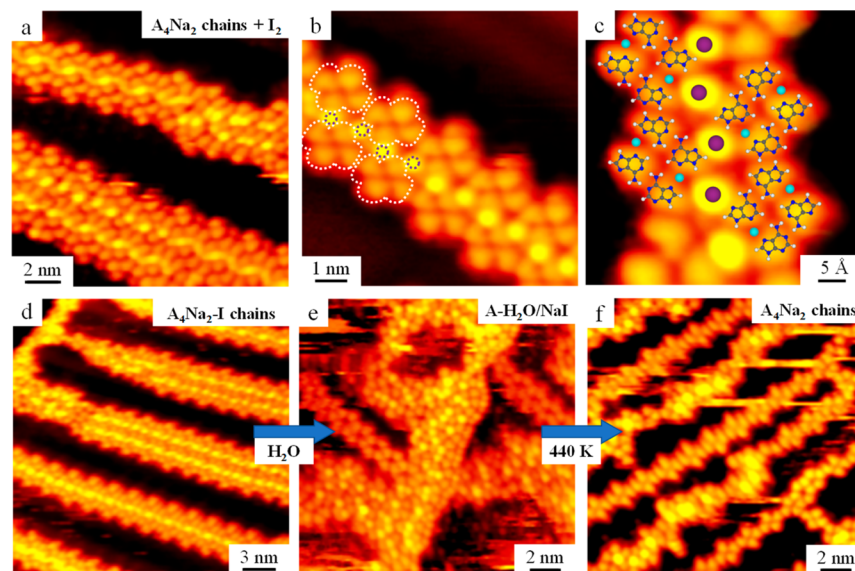


Figure 6. (a–c) Formation of A₄Na₂ chains stitched by iodine on Au(111) formed by direct iodine doping on an A₄Na₂ chains precovered surface. (a) Large-scale and (b) close-up STM images showing the A₄Na₂ chains stitched by iodine. The individual A₄Na₂ motifs and the iodine are depicted by white contours and purple circles, respectively. (c) High-resolution STM image partially superimposed with the structural model. H: white; C: gray; N: blue; Na: light blue. I: purple. (d–f) Formation of A₄Na₂ chains after exposing the A₄Na₂-I chains precovered surface to a water environment and then annealing. (d) STM image showing the A₄Na₂ chains stitched together by iodine. (e) STM image showing the mixture of A-H₂O and NaI after exposing the sample (held at RT) to a water environment at a pressure of ~ 0.001 mbar. (f) STM image showing the formation of individual A₄Na₂ chains after annealing at 440 K.

Moreover, to explore the generality of such a strategy, we perform further studies with the introduction of other sodium halides (*e.g.*, NaBr and NaI). First, we also model the ER process by heating the NaBr and NaI precovered Au(111) surface at different temperatures (from RT to ~ 500 K) under a water environment at a pressure of ~ 0.001 mbar, respectively. It is found that the NaBr and NaI square lattices were also not perturbed and there is no erosion of edges of salt islands (as shown in Figures S3 and S4, respectively), which thus indicates

that the dissolution of NaBr and NaI *via* the ER process seems unfeasible also.

Next, the LH processes of NaBr and NaI dissolution are modeled with the assistance of the A molecules as the water reservoir on the surface. After co-deposition of NaBr and A molecules on the Au(111) surface held at RT, it is observed that the NaBr and A molecules remain separated in their own self-assembled structures (as shown in Figure 4a). After subsequently exposing such a sample (held at RT) to the water

environment at a pressure of ~ 0.001 mbar, it leads to the coexistence of NaBr islands and A-H₂O structures (as shown in Figure 4b). Further annealing the sample to 420 K results in the formation of A₄Na₂ chains and the vanishing of NaBr islands (as shown in Figure 4c) as expected.

To further explore if Br ions are still on the surface or not, we similarly performed the control experiment by simply depositing A and NaBr on the surface and annealing the sample step by step without introduction of water. As shown in Figure 4d–f, it is observed that A and NaBr separated structures transform into the disordered phase after annealing the sample at 420 K, and A molecules desorb from the surface at 450 K, leaving the NaBr islands alone. Such an experiment shows that A and Na⁺ cannot form the A–Na chain structure when Br[−] is present on the surface; instead, due to the strong interaction between Na⁺ and Br[−] (stronger than that between Na⁺ and I[−] but weaker than that between Na⁺ and Cl[−]),³⁵ formation of an A/NaBr mixture is predominant. It is speculated that NaBr should exist in the mixed structure in the form of a Na–Br dimer. On the other hand, it was shown that Br normally desorbs from the Au(111) surface at temperatures above 500 K^{31,32} (also cf. Figure S3). Therefore, it is rational to speculate that water molecules should facilitate the desorption of Br ions from the surface by forming stable Br[−] hydrates. From the above, we could conclude that Br ions should be absent in the situation shown in Figure 4c. Thus, it demonstrates that the dissolution of NaBr through surface-confined water molecules *via* the LH process is achieved.

Finally we discuss the case of the experiment involving NaI. After co-deposition of NaI and A molecules on the Au(111) surface held at RT, it is observed that the NaI and A molecules directly mix with each other (as shown in Figure 5a). After subsequently exposing such a sample (held at RT) to the water environment at a pressure of ~ 0.001 mbar, it leads to the formation of an A–H₂O and NaI mixture phase (as shown in Figure 5b). Further annealing the sample to 440 K results in the formation of A₄Na₂ chains (as shown in Figure 5c), as expected. To further explore if I ions are still on the surface, we also perform a control experiment by simply depositing A and NaI on the surface and annealing the sample step by step without introduction of water. NaI and A molecules directly mix to form the disordered phase (Figure 5d) on Au(111) at RT, and it is able to transform into the ordered multiple chains with thermal treatment at 370 K (Figure 5e). Such an experiment shows that A, Na⁺, and I[−] form the multiple chain structure resembling the single A–Na chains stitched by I[−] due to the even weaker interaction between Na⁺ and I[−] in comparison with that between Na⁺ and Br[−].³⁵ More details on this multiple chain structure are shown in Figure 6. Further annealing the sample at 440 K leads to the destruction of the chains and the formation of the A/NaI mixture phase following the herringbone reconstruction of the Au(111) surface (as shown in Figure 5f). In all, the single A₄Na₂ chain structures (cf. Figure 5c) is hindered due to the presence of I[−].

To further study the multiple chain structure (Figure 5e), a comparative experiment has been performed by introducing iodine to the A₄Na₂ chains, as shown in Figure 6a, which leads to the formation of the same multiple chains as shown in Figure 5e. As shown in the close-up STM image (Figure 6b), the bright protrusions are assigned to the iodine (indicated by purple circles), and the A₄Na₂ motifs are depicted by the white contours. The corresponding structural model partially superimposed on the high-resolution STM image is shown in Figure

6c. After subsequently exposing the A₄Na₂–I chains precovered sample (Figure 6d) to a water environment at a pressure of ~ 0.001 mbar, it leads to the formation of an A–H₂O/NaI mixture (as shown in Figure 6e). Further annealing the sample to 440 K also results in the formation of single A₄Na₂ chains (Figure 6f). Previous studies have shown that iodine normally desorbs from the Au(111) surface at temperatures above 500 K^{33,34} (also cf. Figure S4). Again, it is rational to speculate that water molecules should facilitate the desorption of I ions from the surface by forming the stable I[−] hydrates. From the above, we conclude that the dissolution of NaI through surface-confined water molecules *via* the LH process is achieved.

CONCLUSIONS

In conclusion, with the assistance of A molecules as a water reservoir and carrier, we achieve the dissolution of sodium halides (NaCl, NaBr, NaI) above RT *via* the LH mechanism, along with the selective formation and desorption of stable halide ion hydrates from the Au(111) surface. Such an on-surface salt dissolution is only realized *via* the LH process rather than the ER one. To do so, water molecules confined by adenine molecules is a prerequisite to facilitate the dissolution process. The strategy also offers a facile way to prepare different halide ion hydrates for further studies on the hydration number of these ion hydrates, which may be further related to their configurations and properties. Furthermore, a similar on-surface strategy could be extended to conventional insoluble salts, for example, silver chloride (AgCl), which may allow us to gain fundamental insight into the mechanism of solubility by surface science methods.

METHODS

All STM experiments were performed in a UHV chamber (base pressure 1×10^{-10} mbar) equipped with a variable-temperature, fast-scanning “Aarhus-type” STM using electrochemically etched W tips purchased from SPECS,^{36,37} a molecular evaporator, and an e-beam evaporator, and other standard instrumentation for sample preparation. The Au(111) substrate was prepared by several cycles of 1.5 keV Ar⁺ sputtering followed by annealing to 800 K for 15 min, resulting in clean and flat terraces separated by monatomic steps. The adenine molecule (from Sigma-Aldrich (purity >99%) and NaCl, NaBr, and NaI salts (from Sigma-Aldrich, purity >99%) were loaded into different glass crucibles in the molecular evaporator. After a thorough degassing, the A molecules and salts were deposited onto the Au(111) surface by thermal sublimation. The alkali metal sodium was evaporated from Alvasource (from Alvac) *via* conventional resistance heating after fully degassing. Pure deionized water (from Sigma-Aldrich) was loaded in a dosing tube positioned in the preparation chamber and further purified under vacuum by several freeze–thaw cycles to remove remaining impurities.³⁸ Water molecules were then continuously dosed *in situ* onto the Au(111) surface held at room temperature through a leak valve at a pressure from 10^{-5} to 10^{-3} mbar. I₂ (from Sigma-Aldrich, purity >99%) was dosed *in situ* onto the surface through a leak valve at a pressure of $\sim 10^{-7}$ mbar. The sample was thereafter transferred within the UHV chamber to the STM, where measurements were carried out at ~ 150 K. All of the STM images were further smoothed to eliminate noises. Scanning conditions: $I_t = 0.5$ – 0.8 nA, $V_t \approx -1200$ mV.

The calculations were performed in the framework of DFT by using the Vienna *ab initio* simulation package (VASP).^{39,40} The projector-augmented wave method was used to describe the interaction between ions and electrons;^{41,42} the Perdew–Burke–Ernzerhof generalized gradient approximation exchange–correlation functional was employed,⁴³ and van der Waals interactions were included using the dispersion-corrected DFT–D3 method of Grimme.⁴⁴ The atomic structures were relaxed using the conjugate

gradient algorithm scheme as implemented in the VASP code until the forces on all unconstrained atoms were ≤ 0.03 eV/Å. The simulated STM images were obtained by the Hive program based on the Tersoff–Hamann method.^{45,46}

ASSOCIATED CONTENT

Supporting Information

The Supporting Information is available free of charge on the ACS Publications website at DOI: 10.1021/acsnano.9b02259.

STM image of the coexistence of adenine and NaCl islands together with A_4Na_2 chains during the NaCl dissolution process; DFT-optimized models of the $A-H_2O-Cl$ lever; STM images of the undissolved NaBr and NaI on Au(111) during the ER process (PDF)

AUTHOR INFORMATION

Corresponding Author

*E-mail: xuwei@tongji.edu.cn.

ORCID

Wei Xu: 0000-0003-0216-794X

Notes

The authors declare no competing financial interest.

ACKNOWLEDGMENTS

The authors acknowledge financial support from the National Natural Science Foundation of China (21622307, 21790351) and the Fundamental Research Funds for the Central Universities. Aidi Zhao is acknowledged for providing the Na source.

REFERENCES

- (1) Wellman, H. W.; Wilson, A. T. Salt Weathering, a Neglected Geological Erosive Agent in Coastal and Arid Environments. *Nature* **1965**, *205*, 1097–1098.
- (2) Johnson, K. S. Dissolution of Salt on the East Flank of the Permian Basin in the Southwestern U.S.A. *Dev. Water Sci.* **1982**, *16*, 75–93.
- (3) Hussain, T. M.; Chandrasekhar, T.; Hazara, M.; Sultan, Z.; Saleh, B. K.; Gopal, G. R. Recent Advances in Salt Stress Biology - a Review. *Biotechnol. Mol. Biol. Rev.* **2008**, *3*, 8–13.
- (4) Kurtz, T. W.; DiCarlo, S. E.; Pravenec, M.; Morris, R. C. Changing Views on the Common Physiologic Abnormality That Mediates Salt Sensitivity and Initiation of Salt-Induced Hypertension: Japanese Research Underpinning the Vasodysfunction Theory of Salt Sensitivity. *Hypertens. Res.* **2019**, *42*, 6–18.
- (5) Shalev, E.; Lyakhovskiy, V.; Yechieli, Y. Salt Dissolution and Sinkhole Formation Along the Dead Sea Shore. *J. Geophys. Res.* **2006**, *111*, B03102.
- (6) Gouaux, E.; Mackinnon, R. Principles of Selective Ion Transport in Channels and Pumps. *Science* **2005**, *310*, 1461–1465.
- (7) Payandeh, J.; Scheuer, T.; Zheng, N.; Catterall, W. A. The Crystal Structure of a Voltage-Gated Sodium Channel. *Nature* **2011**, *475*, 353–358.
- (8) Cohen-Tanugi, D.; Grossman, J. C. Water Desalination Across Nanoporous Graphene. *Nano Lett.* **2012**, *12*, 3602–3608.
- (9) Armand, M.; Endres, F.; MacFarlane, D. R.; Ohno, H.; Scrosati, B. Ionic-Liquid Materials for the Electrochemical Challenges of the Future. *Nat. Mater.* **2009**, *8*, 621–629.
- (10) Yamada, Y.; Usui, K.; Sodeyama, K.; Ko, S.; Tateyama, Y.; Yamada, A. Hydrate-Melt Electrolytes for High-Energy-Density Aqueous Batteries. *Nat. Energy* **2016**, *1*, 16129.
- (11) Verdager, A.; Sacha, G. M.; Bluhm, H.; Salmeron, M. Molecular Structure of Water at Interfaces: Wetting at the Nanometer Scale. *Chem. Rev.* **2006**, *106*, 1478–1510.

(12) Garcia-Manyes, S.; Verdager, A.; Gorostiza, P.; Sanz, F. Alkali Halide Nanocrystal Growth and Etching Studied by AFM and Modeled by MD Simulations. *J. Chem. Phys.* **2004**, *120*, 2963–2971.

(13) Verdager, A.; Segura, J. J.; Fraxedas, J.; Bluhm, H.; Salmeron, M. Correlation between Charge State of Insulating NaCl Surfaces and Ionic Mobility Induced by Water Adsorption: a Combined Ambient Pressure X-Ray Photoelectron Spectroscopy and Scanning Force Microscopy Study. *J. Phys. Chem. C* **2008**, *112*, 16898–16901.

(14) Yang, Y.; Meng, S.; Xu, L. F.; Wang, E. G.; Gao, S. Dissolution Dynamics of NaCl Nanocrystal in Liquid Water. *Phys. Rev. E* **2005**, *72*, No. 012602.

(15) Liu, L.-M.; Laio, A.; Michaelides, A. Initial Stages of Salt Crystal Dissolution Determined with *Ab Initio* Molecular Dynamics. *Phys. Chem. Chem. Phys.* **2011**, *13*, 13162–13166.

(16) Klimeš, J.; Bowler, D. R.; Michaelides, A. Understanding the Role of Ions and Water Molecules in the NaCl Dissolution Process. *J. Chem. Phys.* **2013**, *139*, 234702.

(17) Peng, J.; Cao, D.; He, Z.; Guo, J.; Hapala, P.; Ma, R.; Cheng, B.; Chen, J.; Xie, W. J.; Li, X.-Z.; et al. The Effect of Hydration Number on the Interfacial Transport of Sodium Ions. *Nature* **2018**, *557*, 701–705.

(18) Peng, J.; Guo, J.; Ma, R.; Meng, X.; Jiang, Y. Atomic-Scale Imaging of the Dissolution of NaCl Islands by Water at Low Temperature. *J. Phys.: Condens. Matter* **2017**, *29*, 104001.

(19) Weinberg, W. H. *Kinetics of Surface Reactions*; Rettner, C. T., Ashfold, M. N. R., Eds.; Royal Society of Chemistry: Cambridge, London, UK, 1991; p 171.

(20) Rettner, C. T. Reaction of an H-Atom Beam with Cl/Au(111): Dynamics of Concurrent Eley-Rideal and Langmuir-Hinshelwood Mechanisms. *J. Chem. Phys.* **1994**, *101*, 1529–1546.

(21) Cacciatore, M.; Rutigliano, M.; Billing, G. D. Eley-Rideal and Langmuir-Hinshelwood Recombination Coefficients for Oxygen on Silica Surfaces. *J. Thermophys. Heat Transfer* **1999**, *13*, 195–203.

(22) Zhang, C.; Xie, L.; Wang, L.; Kong, H.; Tan, Q.; Xu, W. Atomic-Scale Insight into Tautomeric Recognition, Separation, and Interconversion of Guanine Molecular Networks on Au(111). *J. Am. Chem. Soc.* **2015**, *137*, 11795–11800.

(23) Xie, L.; Zhang, C.; Ding, Y.; E, W.; Yuan, C.; Xu, W. Structural Diversity of Metal-Organic Self-Assembly Assisted by Chlorine. *Chem. Commun.* **2017**, *53*, 8767–8769.

(24) Shimizu, T. K.; Jung, J.; Imada, H.; Kim, Y. Supramolecular Assembly Through Interactions between Molecular Dipoles and Alkali Metal Ions. *Angew. Chem., Int. Ed.* **2014**, *53*, 13729–13733.

(25) Skomski, D.; Abb, S.; Tait, S. L. Robust Surface Nano-Architecture by Alkali-Carboxylate Ionic Bonding. *J. Am. Chem. Soc.* **2012**, *134*, 14165–14171.

(26) Stacchiola, D.; Park, J. B.; Liu, P.; Ma, S.; Yang, F.; Starr, D. E.; Muller, E.; Sutter, P.; Hrbek, J. Water Nucleation on Gold: Existence of a Unique Double Bilayer. *J. Phys. Chem. C* **2009**, *113*, 15102–15105.

(27) Lucht, K.; Loose, D.; Ruschmeier, M.; Strotkotter, V.; Dyker, G.; Morgenstern, K. Hydrophilicity and Microsolvation of an Organic Molecule Resolved on the Sub-Molecular Level by Scanning Tunneling Microscopy. *Angew. Chem., Int. Ed.* **2018**, *57*, 1266–1270.

(28) Zhang, C.; Xie, L.; Ding, Y.; Xu, W. Scission and Stitching of Adenine Structures by Water Molecules. *Chem. Commun.* **2018**, *54*, 771–774.

(29) Kelly, R. E. A.; Xu, W.; Lukas, M.; Otero, R.; Mura, M.; Lee, Y.-J.; Lægsgaard, E.; Stensgaard, I.; Kantorovich, L. N.; Besenbacher, F. An Investigation into the Interactions between Self-Assembled Adenine Molecules and a Au(111) Surface. *Small* **2008**, *4*, 1494–1500.

(30) Lauwaet, K.; Schouteden, K.; Janssens, E.; Van Haesendonck, C.; Lievens, P.; Trioni, M. I.; Giordano, L.; Pacchioni, G. Resolving All Atoms of an Alkali Halide via Nanomodulation of the Thin NaCl Film Surface Using the Au(111) Reconstruction. *Phys. Rev. B: Condens. Matter Mater. Phys.* **2012**, *85*, 245440.

(31) Cai, J.; Ruffieux, P.; Jaafar, R.; Bieri, M.; Braun, T.; Blankenburg, S.; Muoth, M.; Seitsonen, A. P.; Saleh, M.; Feng, X.;

et al. Atomically Precise Bottom-Up Fabrication of Graphene Nanoribbons. *Nature* **2010**, *466*, 470–473.

(32) Björk, J.; Hanke, F.; Stafström, S. Mechanisms of Halogen-Based Covalent Self-Assembly on Metal Surfaces. *J. Am. Chem. Soc.* **2013**, *135*, 5768–5775.

(33) Rastgoo-Lahrood, A.; Lischka, M.; Eichhorn, J.; Samanta, D.; Schmittl, M.; Heckl, W. M.; Lackinger, M. Reversible Intercalation of Iodine Monolayers between On-Surface Synthesised Covalent Polyphenylene Networks and Au(111). *Nanoscale* **2017**, *9*, 4995–5001.

(34) Yao, X.; Xie, L.; Ding, Y.; Wang, X.; Yuan, C.; Xu, W. Iodine-Induced Structural Transformations of Co-Phthalocyanine on Au(111). *J. Phys. Chem. C* **2018**, *122*, 22959–22964.

(35) Cohen, A. J.; Gordon, R. G. Theory of the Lattice Energy, Equilibrium Structure, Elastic Constants, and Pressure-Induced Phase Transitions in Alkali-Halide Crystals. *Phys. Rev. B* **1975**, *12*, 3228–3241.

(36) Besenbacher, F. Scanning Tunneling Microscopy Studies of Metal Surfaces. *Rep. Prog. Phys.* **1996**, *59*, 1737–1802.

(37) Lægsgaard, E.; Österlund, L.; Thostrup, P.; Rasmussen, P. B.; Stensgaard, I.; Besenbacher, F. A High-Pressure Scanning Tunneling Microscope. *Rev. Sci. Instrum.* **2001**, *72*, 3537–3542.

(38) Chen, J.; Guo, J.; Meng, X.; Peng, J.; Sheng, J.; Xu, L.; Jiang, Y.; Li, X. Z.; Wang, E. G. An Unconventional Bilayer Ice Structure on a NaCl (001) Film. *Nat. Commun.* **2014**, *5*, 4056.

(39) Kresse, G.; Hafner, J. *Ab Initio* Molecular Dynamics for Open-Shell Transition Metals. *Phys. Rev. B: Condens. Matter Mater. Phys.* **1993**, *48*, 13115–13118.

(40) Kresse, G.; Furthmüller, J. Efficient Iterative Schemes for *Ab Initio* Total-Energy Calculations Using a Plane-Wave Basis Set. *Phys. Rev. B: Condens. Matter Mater. Phys.* **1996**, *54*, 11169–11186.

(41) Blöchl, P. E. Projector Augmented-Wave Method. *Phys. Rev. B: Condens. Matter Mater. Phys.* **1994**, *50*, 17953–17979.

(42) Kresse, G.; Joubert, D. From Ultrasoft Pseudopotentials to the Projector Augmented-Wave Method. *Phys. Rev. B: Condens. Matter Mater. Phys.* **1999**, *59*, 1758–1775.

(43) Perdew, J. P.; Burke, K.; Ernzerhof, M. Generalized Gradient Approximation Made Simple. *Phys. Rev. Lett.* **1996**, *77*, 3865–3868.

(44) Grimme, S.; Antony, J.; Ehrlich, S.; Krieg, H. A Consistent and Accurate *Ab Initio* Parametrization of Density Functional Dispersion Correction (DFT-D) for the 94 Elements H-Pu. *J. Chem. Phys.* **2010**, *132*, 154104.

(45) Tersoff, J.; Hamann, D. R. Theory of the Scanning Tunneling Microscope. *Phys. Rev. B: Condens. Matter Mater. Phys.* **1985**, *31*, 805–813.

(46) Vanpoucke, D. E. P.; Brocks, G. Formation of Pt-Induced Ge Atomic Nanowires on Pt/Ge(001): a Density Functional Theory Study. *Phys. Rev. B: Condens. Matter Mater. Phys.* **2008**, *77*, 241308.